Surface Roughness Analysis, Modelling and Prediction in Fused Deposition Modelling Additive Manufacturing Technology

Yusuf S. Dambatta, Ahmed A. D. Sarhan

Abstract—Fused deposition modelling (FDM) is one of the most prominent rapid prototyping (RP) technologies which is being used to efficiently fabricate CAD 3D geometric models. However, the process is coupled with many drawbacks, of which the surface quality of the manufactured RP parts is among. Hence, studies relating to improving the surface roughness have been a key issue in the field of RP research. In this work, a technique of modelling the surface roughness in FDM is presented. Using experimentally measured surface roughness response of the FDM parts, an ANFIS prediction model was developed to obtain the surface roughness in the FDM parts using the main critical process parameters that affects the surface quality. The ANFIS model was validated and compared with experimental test results.

Keywords—Surface roughness, fused deposition modelling, adaptive neuro fuzzy inference system, ANFIS, orientation.

I. INTRODUCTION

ADDITIVE Manufacturing (AM) process is a machining technology which is classified into seven different categories: binder jetting, directed energy deposition, material extrusion, material jetting, powder bed fusion, sheet lamination, and vat polymerization. This classification of the AM process gives the basis of selectively extruding the build material through the nozzle of a heating element, this led to the development of the FDM process [1].

At the time of its discovery, the FDM process was involved mainly on modelling of prototypes for visualizations and testing of products properties prior to mass productions. Recently, the process has been advanced into an alternative method for production of various functional end use parts directly from the CAD data. Recent advancements in AM has also seen the FDM process used in constructing conceptual models and functional parts from polymers, metal and ceramics. The fabrication process has seen a great deviation from a mere tool for visualizations and testing purposes, to manufacturing of fully functional products [2], [3].

Despite the numerous benefits of the FDM process, it is yet encompassed with various kinds of setbacks such as poor

Yusuf Suleiman Dambatta is with the Center of Advanced Manufacturing and Material Processing, Department of Mechanical Engineering, Faculty of Engineering, University of Malaya, Kuala Lumpur, 50603, Malaysia (Corresponding author phone: +60146453582; e-mail: ysidambatta@yahoo.com).

Ahmed. A.D. Sarhan is an associate professor at the Department of Mechanical Engineering, Faculty of Engineering, University of Malaya, Kuala Lumpur, 50603, Malaysia (e-mail: ah_sarhan@um.edu.my).

surface quality, strength of products etc. The poor surface quality observed in end products of the FDM process was largely due to the layer upon layer deposition of the building process. Investigations have confirmed that there are three types of surface textures in the FDM prototypes. The bottom surface is made up of the first deposited layer, which is usually in direct contact with the printing platform or support material. Hence, it picks up the surface texture of the build platform (or the support material which had been deposited already). Similarly, the top layer is the last layer to be deposited, it usually consists of a ridged surface which results from the structure of the strands of the modelling material. The third texture observed was the middle surface which takes the rough texture of the layer upon layer pattern [4].

Several investigations were done in order to improve the part quality by adequately building a prediction model of the surface roughness in the FDM parts. Boschetto et al. [5] used experimental analysis to diversify the robustness in predicting the surface roughness in FDM process. They focused on prediction of the surface roughness around the FDM models using a feed forward artificial neural network, this led to a significant improvement in predicting the surface roughness within the ranges of 0^{0} - 30^{0} and 150^{0} - 180^{0} . Garg et al. [6] used a different approach on the analysis of the FDM output properties such as surface roughness, hardness of prototypes, dimensional accuracy, build cost, etc. They analysed the FDM process using the hybrid M5_genetic programming (M5_GP) with the aim of comparing this method with other modelling systems such as support vector regression (SVR) and also the adaptive neuro-fuzzy inference system (ANFIS). The research done was used to obtain an optimized model for the output of the FDM processed parts such as surface roughness, hardness, economic impacts, and also time of building of the prototypes. By optimizing the input process parameters such as layer thickness, orientation, raster angle, road width and angle of deposition, an optimized model for predicting surface roughness using process parameters. It was observed that the hybrid M5 genetic programming model was optimal as compared to the SVR models. Also, Anitha et al. [7] used Taguchi method to investigate the effects of layer thickness, raster width and deposition speed on the surface roughness of FDM parts. They realised that layer thickness is the most significant process parameter which affects surface roughness of the FDM prototypes.

Sun et al. [8] studied the effects of the FDM process parameters on processing times, surface quality and strength of the FDM prototypes. They realised that the temperature history of the preceding layer interfaces significantly affects the quality of the bond formed with newly deposited layers. The results from their experiments shows that the temperature of the building chamber affects the surface finish of the built model. They recommended that there should be some automatic cooling methods for the layers so as to improve the physical properties of the final prototypes in the FDM process. In the same vain, it was observed that different areas across the FDM layers tend to undergo asymmetric thermal deteriorations due to different deposition styles. The topmost layer was observed to also have less bonding gradient like the other layers, this is due to the lack of an all-round heat

distributions present in the layers. Boschetto et al. [5] developed a prediction model for surface roughness using the process parameters of the FDM process. Their hypothetical model was realised to be effective in the prediction of the best raster orientation for optimal surface quality.

The preceding review confirms the existence of the physical deficiency obtainable in the FDM prototypes, most of which occur as a result of the model deposition patterns. It is also affirmed that the process parameters significantly affect the outcome of the surface quality of the FDM prototypes. In this research, an ANFIS model for determining the surface roughness in the FDM prototypes will be developed. This model can be used to effectively determine the surface roughness values in the FDM prototypes containing hollow slots at optimized raster orientations and layer thickness.

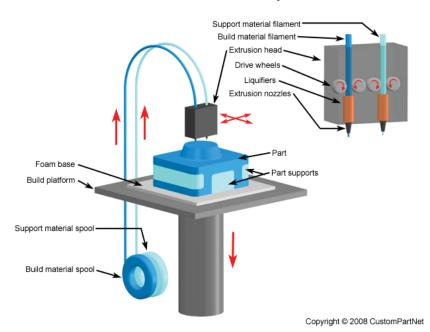


Fig. 1 FDM [12]



Fig. 2 Dimension SST 1200es FDM machine crest ultrasonic generator [12]

II. EQUIPMENT AND METHOD

FDM was first developed by stratasys, it involved fabrication of a geometric model by depositing layer upon layer filaments of thermoplastics such as ABS, nylon, polyethylene, polypropylene etc. The temperature controlled

extrusion nozzles are continually fed with the polymer material, the material is liquefied by the heat of the extrusion nozzles and then first layer is strategically extruded onto the build platform, the subsequent layers are then deposited on their preceding layers along the z-axis. The build environment is kept at an envelope temperature of 78 °C, while the temperature of the extrusion nozzle is 300 °C, this makes the extruded material to re-solidify upon deposition on the build platform [9]-[11]. The FDM machine consists of an in-built computer numerical control (CNC) system which moves the extrusion head along the x-y direction to deposit the desired layer as depicted in Fig. 1. The samples were fabricated using Stratasys "Dimension SST 1200es". This machine is made up of 406 mm × 355 mm × 406 mm fabrication chamber. The model material used is the P430 ABSplus Ivory model and the support material used is the ABS polymer. After each layer is deposited, the build platform lowers downwards and the

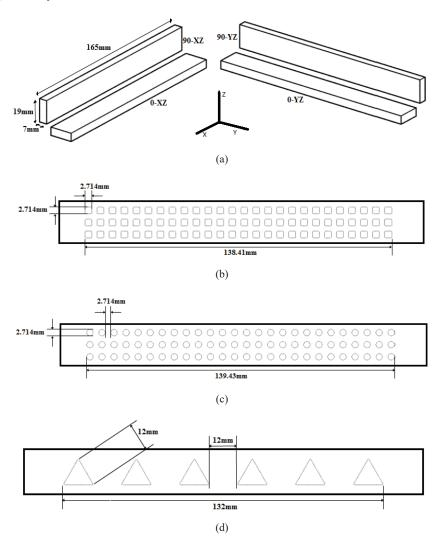
process of depositing a new layer upon the previous layer begins. The support materials are also deposited in places with overhangs and hollows simultaneously with the build materials. The support material can be detached by manual operation or ultrasonic cleaning in the post processing stage using the crest ultrasonic machine shown in Fig. 2.

III. EXPERIMENTATION

The manufacturing process involves a series of steps ranging from the CAD model design to the post processing stage. In order to build the prediction model for the surface roughness of the FDM process, the CATIA V5 software was used to design five different cuboid models (see Fig. 3). These models were designed with different geometries of hollow shapes as found in [11].

The respective STL files of the 3D models were processed into sliced forms using the CatalystEXTM software and were prepared for manufacturing using the FDM machine. Stratasys FDM dimension SST1200es machine was used in fabricating the specimens, the part fill style was selected as solid fill, and

the material utilized is the (ABS P400) Acrylonitrile Butadiene Styrene polymer. The melting temperature was set at 300 °C and the filament was deposited via the extrusion nozzle onto a plastic platform and the envelope temperature was set as 78 °C. Two layer thickness settings were used in this experiment (0.254 mm and 0.3301 mm), and four angular orientations were utilized as shown in Table I. The surface roughness measurements were taken using the mitutoyo SJ210 profilometer with the direction of measurement being perpendicular to the pattern of deposition. The three different textures are illustrated in Fig. 3 (f), the top plane is the side corresponding to deposition orientation, and the bottom plane is the direct opposite of the top plane and it in contact with the build platform. Moreover, the sides are the regions which take up the texture of the layer upon layer arrangement. In the samples containing hollow structures, the roughness values were taken at the edges of the hollows, this was used to check the effects of the observed deformations on the surface quality of the prototypes.



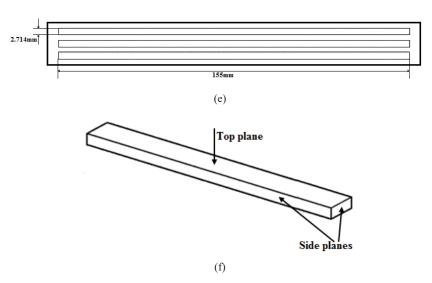


Fig. 3 Example of CAD designed models (a) building orientation for full solid samples (b) building orientation for square hollow samples (c) building orientation for circular hollow samples (d) building orientation for the triangular hollow samples and (e) building orientation for long stripes (f) planes of the samples

TABLE I EXPERIMENTAL SET-UP

EXI EXIMENTAL DEL CI						
Sr. no.	Factors	Level 1	Level 2	Level 3	Level 4	Level 5
1	Layer thickness (mm)	0.2540	0.3302	-	-	-
2	orientation (degree)	0-XZ	90-XZ	0-YZ	90-YZ	-
3	Geometry	Square hollow	Circular hollow	Angular hollow	Long stripe	Full solid

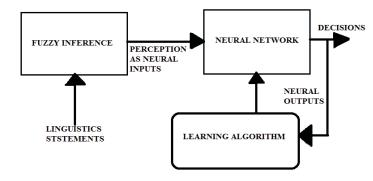


Fig. 4 (a) Neuro-fuzzy system [15]

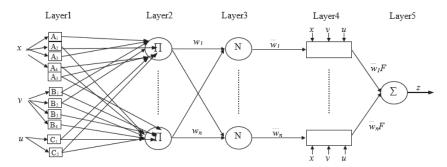


Fig. 4 (b) ANFIS architecture for Sugeno fuzzy model

IV. ANFIS MODELLING

The ANFIS model is used to integrate the artificial cognitive reasoning like that of a human brain onto a fuzzy logic. The predictability of the fuzzy neural system is developed in accordance with neural morphology of biological systems, which is then validated using Mamdani control model during learning process, and the fuzzy inference is built as shown in Fig. 4 (a) [13], [14]. This system uses a feedforward propagation system which is divided into several layers modelled as the learning algorithm as shown in Fig. 4 (b). The ANFIS model for the prediction of surface roughness in FDM process was the constructed using the MATLAB software.

In this work, the layer thickness, angular orientation and weighted geometrical model were utilised as the inputs of the ANFIS model, while the surface roughness was utilised as the outputs of the model [15]. The gbellmf function was used due to the non-linear relationship between the input and output variables. An example of the rules used in this work has the form:

If Input
$$1 = x$$
 and Input $2 = y$,
THEN Output is $z = ax + by + c$

The ANFIS prediction model built in this work performs well in training and learning. After 10 epochs, the average mean prediction error of the model was about 0.000006161 and the average mean verification error of 0.000009523. The learning curve shown in Fig. 5 shows a drastic sloping and steady convergence after about 3-epochs.

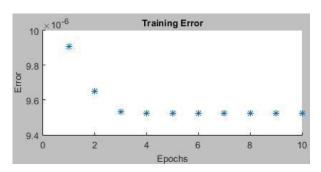


Fig. 5 Training algorithm

V. RESULTS AND DISCUSSION

The results of surface roughness from the experimentation process above was then used to construct an ANFIS prediction model which can be used to predict the surface roughness in the FDM prototypes. The three surface profiles realised from the fabricated prototypes can be predicted in the constructed ANFIS model by simply using the parametric settings in the process i.e. layer thickness and orientation angle. The measured experimental surface roughness of the fabricated prototypes was tabulated in Table I, and then used as the input training data for the ANFIS model. By critical analysis of the fabricated FDM parts, it can be observed that the upper surface has the lowest value of surface roughness Ra, while the bottom surface has a slightly higher Ra values compared to the upper region. This differences could be attributed to the

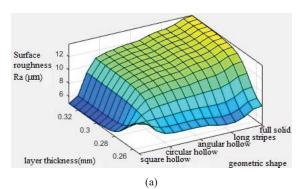
contact which the bottom side makes with the building platform and/or the support material. Furthermore, the effects of the process parameters on the surface roughness of the individual samples were investigated and analysed.

TABLE II SURFACE ROUGHNESS MEASUREMENTS

SURFACE ROUGHNESS MEASUREMENTS							
Exp.	Run	Sample name	Orient.	Thicknes	Surface	roughness	Ra (µm)
No.	No.			S	Upper	Bottom	Side
					plane	plane	planes
1	7	Square hollow	0º XZ	0.254	10.010	14.360	17.375
2	8	Square hollow	90° XZ	0.254	7.503	16.930	16.077
3	17	Square hollow	90° YZ	0.254	7.627	15.000	16.472
4	18	Square hollow	$0^{0}\mathrm{YZ}$	0.254	11.217	17.527	17.070
5	29	Square hollow	$0^0 XZ$	0.332	7.827	13.900	22.393
6	30	Square hollow	90° XZ	0.332	11.373	19.043	21.820
7	39	Square hollow	$90^{\circ} YZ$	0.332	9.113	16.730	22.207
8	40	Square hollow	$0^{0}\mathrm{YZ}$	0.332	6.773	12.320	22.078
9	3	Circular hollow	$0^0 XZ$	0.254	6.307	14.440	17.203
10	4	Circular hollow	90° XZ	0.254	7.253	14.010	16.0920
11	11	Circular hollow	0^0 YZ	0.254	6.563	12.437	17.027
12	12	Circular hollow	90° YZ	0.254	6.777	12.500	15.902
13	23	Circular hollow	0^0 XZ	0.332	7.767	14.777	21.942
14	24	Circular hollow	$90^{\circ} XZ$	0.332	12.38	16.927	22.532
15	33	Circular hollow	0^0 YZ	0.332	9.837	14.657	22.815
16	34	Circular hollow	90° YZ	0.332	12.603	13.820	21.667
17	1	Angular hollow	$0^0 XZ$	0.254	6.687	15.187	17.482
18	2	Angular hollow	$90^{\circ} XZ$	0.254	6.840	14.020	17.378
19	9	Angular hollow	0^0 YZ	0.254	6.867	16.133	17.668
20	10	Angular hollow	90° YZ	0.254	7.177	15.130	17.417
21	21	Angular hollow	$0^0 XZ$	0.332	6.767	13.623	22.360
22	22	Angular hollow	$90^{\circ} XZ$	0.332	10.943	16.563	22.365
23	31	Angular hollow	0^0 YZ	0.332	12.707	15.313	22.620
24	32	Angular hollow	$90^{\circ} YZ$	0.332	13.037	17.983	23.128
25	13	Long stripes	$0^{0} \mathrm{YZ}$	0.254	7.490	10.997	17.435
26	14	Long stripes	90° YZ	0.254	6.163	13.083	15.670
27	19	Long stripes	90° XZ	0.254	5.170	14.363	16.532
28	20	Long stripes	0^0 XZ	0.254	8.627	13.017	16.973
29	25	Long stripes	0^{0} XZ	0.332	8.607	18.470	22.377
30	26	Long stripes	$90^{\circ} XZ$	0.332	11.363	18.040	21.270
31	35	Long stripes	$0^{0}\mathrm{YZ}$	0.332	14.070	16.900	22.578
32	36	Long stripes	$90^{\circ}\mathrm{YZ}$	0.332	12.293	15.940	20.180
33	5	Full solid	0^0 XZ	0.254	6.613	16.820	17.227
34	6	Full solid	$90^{\circ}\mathrm{XY}$	0.254	7.923	16.217	16.952
35	15	Full solid	$90^{\circ} YZ$	0.254	7.300	12.447	16.657
36	16	Full solid	$0^{0}\mathrm{YZ}$	0.254	7.760	17.073	17.248
37	27	Full solid	0^0 XZ	0.332	9.200	16.680	21.695
38	28	Full solid	$90^{\circ}\mathrm{XY}$	0.332	12.940	23.387	22.372
39	37	Full solid	$90^{\circ} YZ$	0.332	10.380	13.710	22.157
40	38	Full solid	$0^0 \mathrm{YZ}$	0.332	14.640	16.200	22.882

The variation in surface roughness of the upper surface of fabricated samples with respect to the parametric settings are shown in Fig. 6. Fig. 6 (a) illustrates the relationship between the sample geometric shape, the layer thickness and the surface roughness (Ra). It could be observed that there is a steady increase in the surface roughness as the layer thickness was being increased. The smaller layer thickness (0.254 mm) has a lower surface roughness value, and hence the surface roughness could be said to be directly proportional to the layer

thickness. Thus, whenever a better surface quality is desired, the selection of layer thickness to be used in manufacturing should be very small. Moreover, Fig. 6 (b) shows that the 0° orientation along the XZ-axis has the least value of surface roughness. The surface quality is higher in the smaller layer thickness and found to decrease as the layer thickness is being increased. However, a dissimilar trend is observed in the bottom surface where the 0° xz-axis orientation is observed to give a better part quality whenever the higher layer thickness is used during the fabrication. Also, the 0° yz-axis orientation is observed to be directly proportional to the layer thickness as illustrated in Figs. 7 (a), (b).



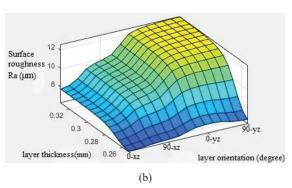
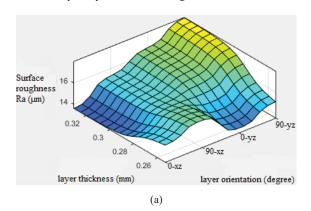


Fig. 6 (a) Variation of surface roughness in the top layer: geometric shape vs layer thickness. (b) Variation of surface roughness in the top layer: layer thickness vs angular orientation



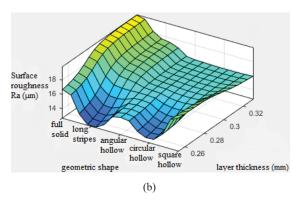
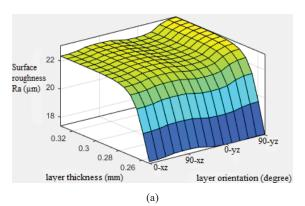


Fig. 7 (a) Variation of surface roughness in the bottom plane: layer thickness vs angular orientation (b) Variation of surface roughness in the bottom layer: geometry vs layer thickness



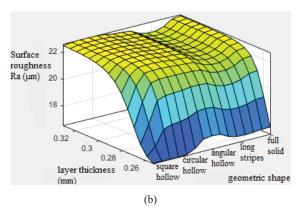


Fig. 8 (a) Variation of surface roughness in the sides layer: layer thickness vs angular orientation (b) Variation of surface roughness in the sides layer: layer thickness vs geometry

The 90° orientation is observed to have a high surface roughness value along all layering directions. On the other hand, the sides region which takes the texture of the layer upon layer arrangement was observed to be independent of the deposition angle (angular orientation). The surface roughness in the sides is found to be directly proportional to the layer thickness, which also corroborates with the findings of previous literatures, see Figs. 8 (a), (b). Furthermore, the hollow structures built using the 90° orientation angle were observed to have deformations e.g. heat affected zones (HAZ)

as shown in Fig. 9. The HAZ occur as a result of contact which exists between the model material and support material. This distortion was observed to greatly affect the surface quality of the FDM parts. The surface texture and straightness of the fabricated prototypes

VI. VERIFICATION

Previous researchers have utilised the standard truncheon test for pyramidal-shaped test [16]-[18], but this work is focused on using the experimental test parts in studying the resultant effect of the layer thickness and deposition angle on the built FDM parts. The aim of the obtaining the surface quality is to be able to present the surface roughness using the input parameters so as to improve the functionality of the FDM prototypes. Here, a set of 10 samples were built for validation purpose, and their resultant surface profiles were used in verifying the performance of the developed ANFIS model. Table III shows the experimental results for the verification data and the results of prediction from the ANFIS model. The ANFIS model was capable of predicting the surface roughness of the prototypes with an average prediction error of about 6.66%. The measured surface roughness was graphically compared with the predicted surface roughness in

Fig. 10, and the constructed ANFIS model can be justified as highly accurate in predictability.

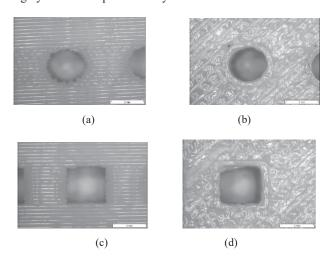


Fig. 9 Surface texture of fabricated prototypes (a) circular hollow fabricated with orientation angle of 90° (b) circular hollow fabricated with orientation angle of 0° (c) square hollow fabricated with orientation angle of 90° (d) square hollow fabricated with orientation angle of 0°

TABLE III SET-UP FOR VERIFICATION SAMPLES

SET-OP FOR VERIFICATION SAMPLES						
Exp. Run no.	Geometry	Orientation (degree)	layer thickness (mm)	Measured surface roughness Ra	Predicted surface roughness Ra (µm)	
1	1	1	0.2540	10.5100	10.0000	
2		4	0.3302	9.6333	9.1100	
3	2	2	0.2540	5.7430	6.5600	
4		2	0.3302	8.5700	9.8400	
5	3	3	0.2540	6.8400	6.8400	
6		1	0.3302	6.9130	6.7700	
7	4	2	0.2540	7.7880	7.4900	
8		4	0.3302	11.4310	12.300	
9	5	3	0.2540	8.3000	7.9200	
10		1	0.3302	8.4260	9.2000	

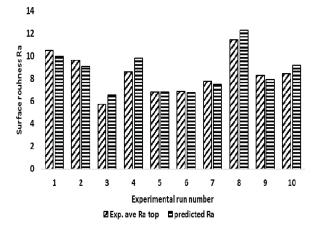


Fig. 10 Experimental measurements vs ANFIS prediction for surface roughness

VII. CONCLUSION

This research involves the development of an ANFIS prediction model for surface roughness in FDM prototypes. The model developed allows for prediction of the surface roughness as a function of the FDM process parameters which includes layer thickness and deposition angle. The experimental response shows that the process parameters deeply affects the surface quality in the FDM prototypes. For cuboid shaped prototypes in full solid mode or containing hollow structures, the surface roughness can be successively obtained using the ANFIS model constructed in this work. The developed model was verified for its predictability of the surface roughness using ten samples of the testing data. It was observed that the ANFIS model constructed for predicting the surface roughness in the FDM prototypes has an accuracy of about 93.34%. The model can be a useful tool when involved in process planning to predict the surface quality prior to manufacturing in other to meet design specifications.

REFERENCES

- [1] Too, M., et al., *Investigation of 3D non-random porous structures by fused deposition modelling*. The International Journal of Advanced Manufacturing Technology, 2002. 19(3): p. 217-223.
- [2] Atzeni, E., et al., Redesign and cost estimation of rapid manufactured plastic parts. Rapid Prototyping Journal, 2010. 16(5): p. 308-317.
- [3] Karapatis, N., J. Van Griethuysen, and R. Glardon, Direct rapid tooling: a review of current research. Rapid Prototyping Journal, 1998. 4(2): p. 77-89.
- [4] Huang, B., Alternate slicing and deposition strategies for Fused Deposition Modelling. 2014, Auckland University of Technology.
- [5] Boschetto, A., V. Giordano, and F. Veniali, 3D roughness profile model in fused deposition modelling. Rapid Prototyping Journal, 2013. 19(4): p. 240-252.
- [6] Garg, A., et al., A hybrid\text {M} 5^\ prime-genetic programming approach for ensuring greater trustworthiness of prediction ability in modelling of FDM process. Journal of Intelligent Manufacturing, 2014. 25(6): p. 1349-1365.
- [7] Anitha, R., S. Arunachalam, and P. Radhakrishnan, Critical parameters influencing the quality of prototypes in fused deposition modelling. Journal of Materials Processing Technology, 2001. 118(1): p. 385-388.
- [8] Sun, Q., et al., Effect of processing conditions on the bonding quality of FDM polymer filaments. Rapid Prototyping Journal, 2008. 14(2): p. 72-80
- [9] Standard, A., F2792-12a.(2012). ". Standard Terminology for Additive Manufacturing Technologies," ASTM International, West Conshohocken. Pa.
- [10] Boschetto, A. and L. Bottini, Roughness prediction in coupled operations of fused deposition modeling and barrel finishing. Journal of Materials Processing Technology, 2015. 219: p. 181-192.
- [11] Sarhan, A.A., et al., Geometrical Structure and Layer Orientation Effects on Strength, Material Consumption and Building Time of FDM Rapid Prototyped Samples. World Academy of Science, Engineering and Technology, International Journal of Mechanical, Aerospace, Industrial, Mechatronic and Manufacturing Engineering, 2015. 9(6): p. 1063-1068.
- [12] www.custompart.net. 2008 (cited 2015 12/10/2015); Available from: http://www.custompartnet.com/wu/images/rapid-prototyping/fdm.png.
- [13] Azar, A.T., Neuro-fuzzy applications in dialysis systems, in Modeling and Control of Dialysis Systems. 2013, Springer. p. 1223-1274.
- [14] Jang, J.-S.R., ANFIS: adaptive-network-based fuzzy inference system. Systems, Man and Cybernetics, IEEE Transactions on, 1993. 23(3): p. 665-695
- [15] Soltan, I.M.A.-R., Surface Roughness Prediction in End-Milling Process. 2008.